Ligand Field Analyses of Tris(biuret)chromium(III) Chloride and Hexaureachromium(III) Bromide

Sung-Jin Park, Byung-Keun Oh, Young-Dong Park,† and Kyu-Wang Lee*

Department of Chemistry and Electronic Materials Research Center, Myongji University, Yongin, Kyonggi-Do 449-728, Korea
†Department of Chemistry, Ajou University, Suwon, Kyonggi-Do 442-749, Korea
Received March 19, 1999

Ligand field analyses for tris(biuret)chromium(III) chloride and hexaureachromium(III) bromide were performed and compared to understand the ligand field properties of both ligands. The optimized $e_{\sigma O}$ and $e_{\pi O}$ values indicate that coordinated oxygen atom in biuret ligand is a moderate σ- and strong π-donor, while that in urea ligand is a weak σ- and moderate π-donor. The electronic structures of those two complexes are quite different and they were well accounted by inclusion of an anisotropic π bonding.

Introduction

The spectroscopic properties of $[Cr(urea)_6]^{3+}$ complex have been extensively studied.[1~8] The close proximity of doublet (^2E_g) and quartet ($^4T_{2g}$) states of this complex give rise to many unusual photophysical properties and these features have not been satisfactorily interpreted. Though the knowledge of ligand field properties and electronic structure is essential to understand this system, its ligand field analysis has been largely neglected, however.

It has been reported that its chelating system, $[Cr(biuret)_3]^{3+}$ exhibit quite different photophysical properties as well as ligand field properties from those of $[Cr(urea)_6]^{3+}$ complex.[9,10] For one instance, $[Cr(biuret)_3]^{3+}$ shows larger ligand field strength and resulting different energy gap between ^2E_g and $^4T_{2g}$ states of the two complexes exhibit discriminatory emission behavior; only phosphorescence is observed in the biuret complex, while phosphorescence-fluorescence dual emissions were observed in the urea complex. Since the symmetry of these complexes is trigonal (D_3), symmetry lowering of biuret complex upon chelation cannot be a major factor for this discrepancy.[9] Moreover, doublet line splittings are more sensitive in urea complex to the subtle geometry changes induced by counter ions. Thus, it is appropriate to analyze and compare the ligand field properties of each ligand to understand the electronic structure of these CrO_6 coordination system.

In this paper, we examined the spectroscopic properties of $[Cr(biuret)_3]^{3+}$ and performed the ligand field analyses of $[Cr(biuret)_3]^{3+}$ and $[Cr(urea)_6]^{3+}$ to elucidate electronic structures and ligand field properties of the ligands. In the framework of the angular overlap model (AOM), the suitability of anisotropic π-bonding was examined in reproducing the unusual doublet splittings in these complexes.

Experimental Section

Tris(biuret)chromium(III) chloride was prepared by a standard method.[10] The needle-shaped, deep green crystals were obtained from successive recrystallization in 0.1M HCl solution in the dark. Luminescence and excitation spectra were measured with a Continuum Nd : YAG laser-pumped dye laser (ND60) and BMI OPO laser as a light source. The emission was analyzed with a CVI 0.5m monochromator (DK480), and was detected with a Hamamatsu R943-02 cooled photomultiplier tube and an SRS boxcar chassis. Microcrystalline samples were mounted on the cold head of a Janis CCS-600 closed cycle He gas cryostat. IR and Raman spectra were measured with a Perkin-Elmer System 2000 FT-IR spectrometer on samples dispersed in Nujol mulls on a polyethylene film (far-IR) or in KBr pellets (mid-IR). Room temperature absorption spectra were recorded with a Shimadzu UV3100 spectrophotometer.

Results and Discussion

Vibrational spectra. The 13K luminescence spectrum of $[Cr(biuret)_3]Cl_3$ is shown in Figure 1. Peaks are rather broad and vibrational side bands are weak, compared to other Cr^{3+} complexes.[5,11] No trace of impurities was detected in temperature and exciting wavelength dependent spectroscopy. The strong peak at 14245 cm^{-1} is coincident with a strong, lowest energy peak in excitation spectrum and

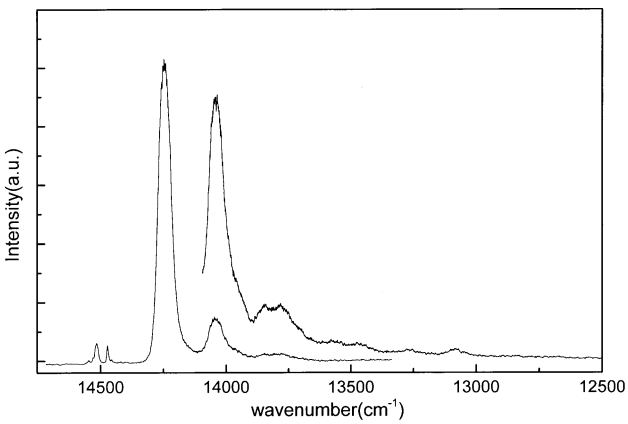

Figure 1. Luminescence spectrum of $Cr(biuret)_3Cl_3$ at 13K.

Table 1. Vibronic intervals in the 13K luminescence spectrum of $[Cr(biuret)_3]Cl_3$

Vibrational Interval(cm^{-1})	IR	Raman	Assignment	$[Cr(urea)_6]^{3+}$ Ref. 5	Biuret Ligand
-297					
-269					
-225			Hot bands		
-208					
-93					
-63					
0			^2E_g origin		
25			Lattice		
67			Lattice		
106	99	102	Rocking or torsion		
	116	114			
210	206	206	(O-Cr-O)	198	
				207	
229	222	226	Sym (O-Cr-O)	226	
				243	
272	264	276	(O-Cr-O)		
	282				
298	298		Asym (Cr-O)	294	
	325	329	(Cr-O)	327	
387	377	383	Sym (Cr-O)	397	
	434	434	Ligand		439
463			229 2 (458)		
	467	465	Ligand		460
	505	505	Ligand		500
685			387 + 298(685)		
769			387 2 (774)		
978					

assigned to the lower energy component of ^2E_g origin. The luminescence spectrum of perchlorate salt is very similar to that of chloride salt and the ^2E_g origin is found at 14227 cm^{-1}.

Vibronic intervals in the luminescence spectrum along with IR and Raman frequencies are listed in Table 1. Though the approximate symmetry of $[Cr(biuret)_3]Cl_3$ is D_3, the actual symmetry is much lower and the symmetry of vibrational modes was not well represented in the two complementary techniques, Raman and IR. The symmetry of vibrational modes was estimated by comparing the relative intensities of the corresponding bands in both spectra. The bands below 250 cm^{-1} correspond to lattice and ligand deformation modes with considerable O-Cr-O bending character. A weak peak at 387 cm^{-1} appears in IR and Raman with considerable intensity and assigned to the symmetric Cr-O stretching mode. A weak peak at 298 cm^{-1} was absent in Raman spectrum and assigned to the asymmetric Cr-O stretching mode. Above 400 cm^{-1}, the frequency of these bands can be found in the free ligand IR spectrum and they are assignable to internal modes of ligands. As seen in Table 1, the frequencies of Cr-O vibration and ligand deformation modes are similar between hexaurea and biuret complexes.

The mid-IR spectrum shows minor frequency changes in most of the biuret ligand vibrations upon complexation with

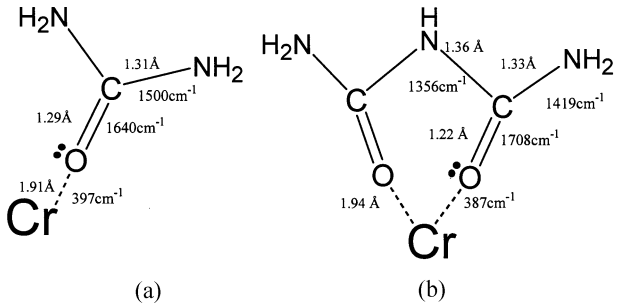

Figure 2. Comparison of IR stretching frequencies and bond lengths (a) $Cr(urea)_6^{3+}$ (b) $Cr(biuret)_3^{3+}$.

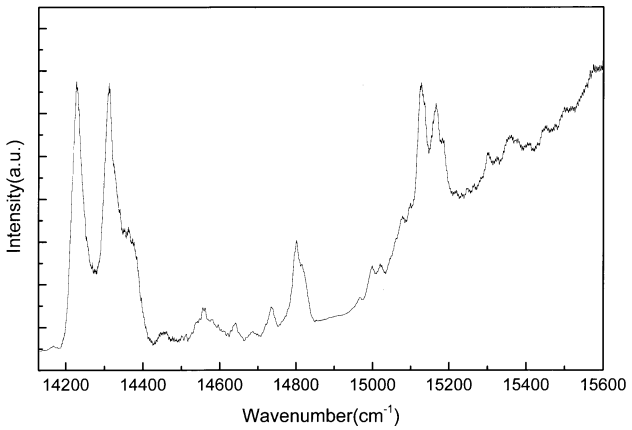

Figure 3. Excitation spectrum of $Cr(biuret)_3Cl_3$ at 13K.

Cr metal, in contrast to the urea complex. The C-N stretching frequencies remain unchanged and the carbonyl stretching frequencies decrease by a few wavenumbers upon complexation in the biuret complex while considerable decrease of ν(C=O) and increase of ν(C-N) frequencies are observed in the urea complex.[12]

The vibrational frequencies and bond lengths of urea and biuret complexes are compared in Figure 2. The x-ray crystal structure of urea suggested the resonance structure of 30% double bond character for the carbon to nitrogen bonds and 40% for the remaining carbon to oxygen bond.[13] Biuret ligand lacks this type of resonance and the double bond character remains mostly in the carbonyl moiety of the ligand.

Electronic spectra. The 12K excitation spectrum of $[Cr(biuret)_3]Cl_3$ is shown in Figure 3 and the peak position and their assignments are tabulated in Table 2. The vibronic lines are also quite attenuated, as seen in the luminescence spectrum. The electronic origins are expected to be quite strong since the effective symmetry of the chromophore is very low. A strong peak at 14245 cm^{-1} coincides with the peak in the luminescence spectrum and is assigned to lower energy component of ^2E_g origin. The other component of ^2E_g origin is found at 14329 cm^{-1}. The 84 cm^{-1} of the ^2E_g splitting is comparable to that of $Cr(urea)_6^{3+}$ complex. Three components of $^4A_{2g} \rightarrow {}^2T_{1g}$ transition can be found with strong intensities at 573, 900, 937 cm^{-1} from the lowest electronic line. As seen in Figure 3, the overlap of the $^2T_{1g}$ transition region with the broad $^4T_{2g}$ band and the consequent

Table 2. Peak positions in the 13K excitation spectrum of [Cr(biuret)$_3$]Cl$_3$. (all data in cm^{-1})

$\bar{\nu}$ - 14245	Assignment	$\bar{\nu}$ - 14245	Assignment
0 s	^2E_g	793 w	$^2T_{1g}$ + 229
29 w,s h	^2E_g+ 25	850 vw	$^2T_{1g}$ + 272
66 vw, sh	^2E_g + 67	871 vw	$^2T_{1g}$ + 298
84 s	$^2E_g'$	900 m	$^2T_{1g}'$
100 vw, sh	^2E_g + 106	937 m	$^2T_{1g}''$
136 w, sh		958 w, sh	$^2T_{1g}$ + 387
228 vw, sh	^2E_g + 229	1008 vw	$^2T_{1g}'$ + 106
274 vw	^2E_g + 272	1018 vw	
284 vw	$^2E_g'$ + 210	1037 vw	$^2T_{1g}''$ + 106
314 vw, sh	$^2E_g'$ + 229	1074 w	
349 w	$^2E_g'$ + 272	1097 vw	$^2T_{1g}'$ + 210
382 vw, sh	^2E_g + 387	1143 w	$^2T_{1g}''$ + 210
412 vw		1151 vw	$^2T_{1g}''$ + 229
469 vw	$^2E_g'$ + 387	1181 vw	$^2T_{1g}'$ + 272
509 vw		1224 w	$^2T_{1g}''$ + 272
573 m	$^2T_{1g}$	1275 vw	$^2T_{1g}'$ + 387
738 vw		1337 vw	$^2T_{1g}''$ + 387
770 w	$^2E_g'$ + 685	1372 vw	$^2T_{1g}'$ + 463

intensity borrowing by the doublet lines are apparent. However, none of the well resolved peaks appear to belong to the $^4T_{2g}$ band. These doublet lines are also observed in room temperature solution absorption and its second derivative spectrum as seen in Figure 4. The components of ^2E_g and $^2T_{1g}$ transitions are located at 14305, 14747 and 15156 cm^{-1} and these support above assignment. The relatively strong band at 20833 cm^{-1} is assigned to the first components of the $^2T_{2g}$ transitions, but the spectrum is not resolved well enough to assign the other components with any certainty.

The broad spin allowed $^4T_{2g}$ and $^4T_{1g}$ bands are observed at 17301 and 23725 cm^{-1}. Split quartet components in D_3 symmetry could not be found even in the second derivative spectrum, while they are found in polarized absorption spectrum of urea complex.[14] It can be explained by the possibility that they are closely located with each other, or the intensity of some components (^4E from $^4T_{2g}$, $^4A_2$ from $^4T_{1g}$, for example) is so weak that they are burried in other components. It is interesting to note that the ligand field strength and effective ligand field symmetry increase with chelation. The quartet bands of biuret complex are shifted to higher energy by about 1200 cm^{-1} relative to those of the hexaureachromium(III) complex.

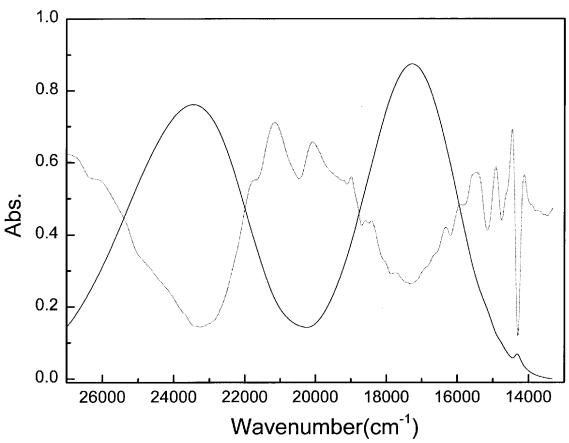

Figure 4. Absorption spectrum (solid line) and second derivative spectrum (dotted line) of Cr(biuret)$_3^{3+}$ in 0.1M HCl solution at room temperature.

Ligand field analysis. Ligand field analyses for [Cr(biuret)$_3$]$^{3+}$ complex as well as hexaurea complex were performed to understand the ligand field properties of the two ligands. The general method of ligand field calculations in the framework of angular overlap model has been described elsewhere.[15,16] The ligand field potential matrix was generated from the six coordinated oxygen atoms, by use of the room temperature X-ray single crystal structure.[9,17~19]

The six parameters varied during the optimization were the AOM ligand field parameters $e_{\sigma O}$ and $e_{\pi O}$, plus interelectronic repulsion parameters *B*, *C* and α_T (the Trees correction parameters), and the spin-orbit coupling parameter, ζ. The π interaction of the oxygen with the metal ion was considered to be anisotropic, confined to the direction perpendicular to the plane defined by the Cr-O-C bonds. The experimental energies used in the fitting process, along with their assignments, are given in Table 3. By variation of six parameters just described, these energies were fit by means of the Powell parallel subspace optimization procedure.[20] The function minimized was

$$F = \sum Q^2 + 10\sum T^2 + 100\sum D^2 + 1000\sum S^2$$

where each term represents a difference between experimental and calculated transition energies or splittings: *D*, the five lowest doublet energies; *T*, the averaged $^2T_2$ peak position; *Q*, the two quartet energies and *S*, the splittings between the doublet energies. The weighting factors in this function are in approximate proportion to the inverse square of the corresponding experimental uncertainty. Reasonable boundary conditions based on the results from other Cr(III) complexes were applied to each parameter, but none of the parameters in the best-fit parameter set approached its boundary value. The optimization was repeated several times with different sets of starting values to confirm that the same global mini-

Table 3. Experimental and calculated transition energies for Cr(biuret)$_3^{3+}$ and Cr(urea)$_6^{3+}$ complex. (all data in cm^{-1})

Cr(biuret)$_3^{3+}$			Cr(urea)$_6^{3+}$		
	Obs.	Calc.[a]		Obs.[c,d]	Calc.[b]
^2E_g	14245	14229	^2E_g	14184	14182
	14329	14348		14265	14265
$^2T_{1g}$	14818	14874	$^2T_{1g}$	14361	14365
	15145	15092		14963	15007
	15182	15152		15129	15108
$^2T_{2g}$	20833	21603	$^2T_{2g}$	20762	20749
$^4T_{2g}$(avg)	17301	17287	$^4T_{2g}$ ^4E	16130[d]	16118
$^4T_{1g}$(avg)	23725	23750	$^4A_1$	17000	17217
			$^4T_{1g}$ ^4E	22570	22306
			$^4A_2$	23400	23133

[a]ligand field parameters: $e_{\sigma o}$ = 7055, $e_{\pi o}$ = 1876, B = 689, C = 2910, T = 106, ζ = 24. [b]$e_{\sigma o}$ = 6200, $e_{\pi o}$ = 1406, B = 676, C = 3121, T = 156, ζ = 194. [c]spectrum of bromide salt, Ref. 5. [d]Ref. 14.

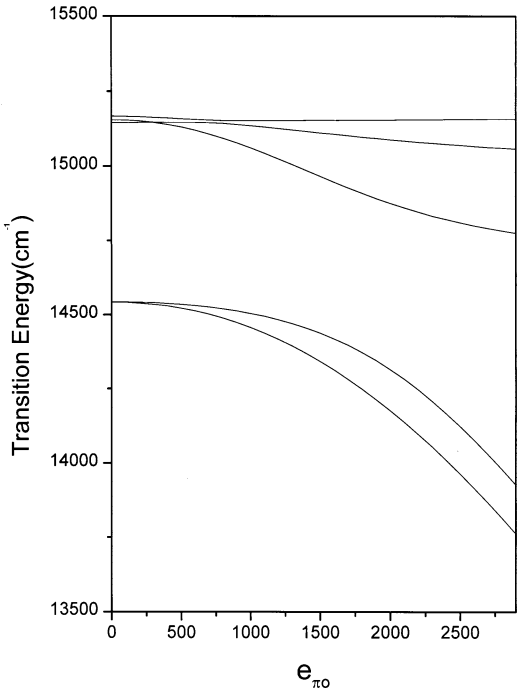

Figure 5. Calculated variation of the transition energies to the ^2E_g and $^2T_{1g}$ state for $Cr(biuret)_3^{3+}$ as a function of $e_{\pi o}$.

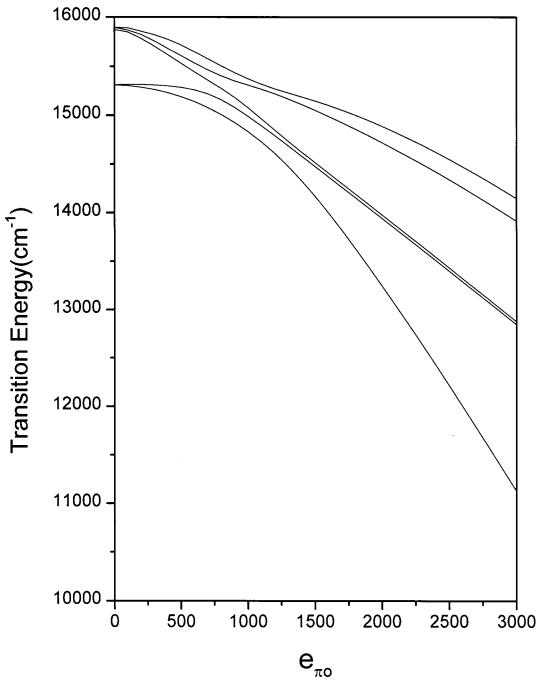

Figure 6. Calculated variation of the transition energies to the ^2E_g and $^2T_{1g}$ states for $Cr(urea)_6^{3+}$ as a function of $e_{\pi o}$.

mum was found.

The results of the optimization and the parameter set used to generate the best-fit energies are listed in Table 3. The optimized $e_{\sigma O}$ and $e_{\pi O}$ values indicate that coordinated oxygen atom in biuret ligand is a medium σ- and strong π-donor, while that in urea ligand is a weak σ- and medium π-donor. It is in accordance with the results of x-ray crystal structure and vibrational analysis, as mentioned in previous section. The electron density is lower in carbonyl moiety of the urea ligand than that of a biuret since urea involves considerable resonance hybrid. The σ-bonding contribution is judged to be more important in determining the ligand field strength of ligands.

Table 3 presents Flint's data for urea complex, which are noteworthy for the large overall doublet splittings, especially in $^2T_{1g}$ region, and the close proximity of ^2E_g and $^2T_{1g}$ states. This is quite surprising since we expect symmetry is lowered upon chelation and larger overall splitting in biuret complex is expected. Indeed, molecular symmetry of biuret complex is lower than that of hexaurea complex.[9] However, both urea and biuret are non-linear ligand and the orientation of their π orbital may affect the metal d orbital energies significantly. By close inspection of x-ray crystal data, the biuret complex shows the π orbital orientation angle ψ to be 40°, which implies pseudoisotropic π-bonding, while the urea complex shows anisotropic π-bonding in which ψ varies from 58° to 72°. The isotropic condition results when $e_{\pi s}$ is equal to $e_{\pi c}$ at $\psi = 45°$, since the overlap of the ligand π orbital with metal d_{xz} and d_{yz} orbitals is then equal.[13]

This geometric difference leads to a quite different behavior of the doublet transitions. Figures 5 and 6 show the calculated behavior of the doublet transition energies as a function of the extent of anisotropic π-bonding of biuret and urea complexes, respectively. The $e_{\sigma o}$ was adjusted to keep the quartet energies approximately constant. The doublet splittings are quite insensitive to the value of e_π in the pseudoisotropic biuret system while doublet splittings become larger and show the considerable mixing between the $^2T_{1g}$ and ^2E_g states as the $e_{\pi o}$ increase in the anisotropic urea system. At $e_{\pi O}$ of around 1500 cm^{-1}, the overall doublet splitting pattern of 1-2-2 is reproduced and fit the experimental data of Flints quite well. The second component of the $^2T_{1g}$ transition located at 14541 cm^{-1} deviate only from calculated energies considerably, however. This may be a vibronic line and the calculated energies suggest that the second component of the $^2T_{1g}$ transition line should be found near 15000 cm^{-1}. The inclusion of an anisotropic bonding markedly improve the fitting and its effect on the doublet line splittings are substantial for these complexes.

Acknowledgment. This work was supported by Korea Science and Engineering Foundation (951-0302-016-2**)** and grant of research instrument support program from Ajou University (1995).

References

1. Porter, G. B.; Schläfer, H. L. *Ber. Bunsenges. Physik. Chem*, **1964**, *68*, 316.
2. Gausmann, H.; Schläfer, H. L. *J. Chem. Phys*. **1968**, *48(9)*, 4056.
3. Dingle, R. *J. Chem. Phys*. **1969**, *50*, 1592.
4. Yersin, H.; Otto, H.; Gliemann, G. *Theor. Chim. Acta*. **1974**, *33*, 63.
5. Flint, C. D.; Palacio, D. J. D. *J.C.S. Faraday II* **1979**, *75*, 1159.

6. Flint, C. D.; Palacio, D. J. D. *J.C.S. Faraday II* **1980**, 76, 82.
7. Yersin, H.; Huber, P.; Gietl, G.; Trümbach, D. *Chem. Phys. Lett* **1992**, *199(1)*, 1.
8. Schmidtke, H. H.; Schoepe, K. E.; Degen, J. *Ber. Bunsenges. Physik. Chem*. **1995**, *99*, 759.
9. Park, S. J.; Lee, K.W.; Park, Y. J. To be published.
10. Chatterjee, K. K.; Porter, G. B. *Inorg. Chem*. **1966**, *5*, 5, 860.
11. Mortensen, O. S. *J. Chem. Phys*. **1967**, *47(10)*, 4215.
12. Penland, R. B.; Mizushima, S.; Curran, C.; Quagliano, J. V. *J. Am. Chem. Soc*. **1957**, *79*, 1575.
13. Vaughan, P.; Donohue, J. *Acta Cryst*. **1952**, *5*, 530.
14. Schönherr, T. *Topics in Curr. Chem*. **1997**, *191*, 87.
15. Hoggard, P. E. *Coord. Chem. Rev.* **1986**, *70*, 85.
16. Lee, K. W.; Eom, K. I.; Park, S. J. *Inorg. Chim. Acta* **1997**, *254*, 131.
17. Davis, P. H.; Wood, J. S. *Inorg. Chem*. **1970**, *9(5)*, 1111.
18. Okaya, Y.; Pepinsky, R. *et al. Acta. Cryst.* **1957**, *10*, 798.
19. Figgis, B. N.; Wadley, L. G. B.; Graham, J. *Acta Cryst.* **1972**, *B28*, 187.
20. Powell, M. J. D. *Comput. J*. **1964**, *7*, 155.